Polym. Bull. (2011) 66:147–164
DOI 10.1007/s00289-010-0317-7

ORIGINAL PAPER

The study on the creep of calcium carbonate-filled polypropylene (PP/$CaCO_3$) prepared at different vibration condition

Ying Lu · Huan Peng · Kaizhi Shen · Zheng Yan

Received: 20 August 2009 / Revised: 25 May 2010 / Accepted: 4 June 2010 /

Abstract A vibration force field had been introduced during the polymer injection processing in the article, which caused some physical properties of the articles were significantly improved. The creep behavior of calcium carbonate-filled polypropylene (PP/$CaCO_3$) prepared at different vibration condition was studied in order to reveal the influence of vibration conditions on the creep behavior. First, the tensile creep behavior of the PP/$CaCO_3$ prepared at different vibration conditions has been investigated with a tensile creep apparatus, and it had been observed that with the vibration frequency increasing, the tensile strain would be maximum value at 0.72 Hz. While the tensile strain of the PP/$CaCO_3$ prepared at different vibration pressure would be decreasing with the vibration pressure increasing. Then the wide-angle X diffraction (WAXD) and the differential scanning calorimeter (DSC) were used to explore the microstructure of the PP/$CaCO_3$ article prepared at different vibration condition. According to the WAXD and DSC data, the number of the crystal grain may play an important role on the change of the creep behaviors of PP/$CaCO_3$ article prepared at different vibration conditions. Finally, the inner reason why the different vibration condition would cause different creep behavior could be found that if the number of the crystal grain is larger, then there would be stronger physical cross-linking structure, which causes stronger anti-creep ability.

Keywords Vibration injection · Tensile creep · Vibration frequency · Vibration pressure amplitude · Crystal grain size

---

Y. Lu · H. Peng · K. Shen · Z. Yan (✉)
The College of Polymer Science and Engineering, Sichuan University, Chengdu 610065, People's Republic of China
e-mail: yanzheng200303@163.com

Introduction

Adding an inorganic filler to a polymer can improve the characteristics, expand the application field, and lower the cost of the polymer products. Therefore, filled polymer systems play a very important role in the engineering plastics. Because of the merits, calcium carbonate has been one of the most widely used fillers in the plastics industry [1–6].

According to the past researches, the mechanical and morphological behavior of a polymer can be changed greatly by introducing the vibration force field during processing. Many vibration techniques and apparatus have been developed to investigate these influences [7–12]. For example, Allen and Bevis [7, 8] used their invention of multi-live feed molding apparatus to introduce shearing oscillation into the melt flow within the cavity, and found that it increased the strength of molded parts and eliminated the effect of weld lines. Ibar [11, 12] introduced vibration field into injection molding when polypropylene (PP) was molded. His results show that the elongation rose 80%, and the yield strength and modulus were also increased greatly.

The research for filling material had also been paid more attention in the past. Luo [13] added a vibration force field in the whole extrusion process, and they found a vibration force field into the whole extrusion process can effectively improve dispersion of nano-particles in the HDPE matrix, cause a smaller particle size and a narrower particle size distribution, and improve mechanical properties. Qu [14, 15] used an electromagnetic dynamic injection molding machine to study the mechanical properties and morphological behavior of calcium carbonate-filled polypropylene (PP/$CaCO_3$), and the tensile stress and the impact stress increase nonlinearly with vibration amplitude and frequency increasing. Moreover, the tensile stress reached a maximum value at about 8 Hz and 0.15 mm for neat PP and PP filled with 3, 20, and 30 wt% $CaCO_3$. For PP filled with 40 wt% $CaCO_3$, the tensile stress reached a maximum value at about 12 Hz and 0.2 mm. The impact stress reached a maximum value at about 12 Hz. On the other hand, Shen [16] investigated the PP/nano-$CaCO_3$ samples by a mechanical vibration injection molding equipment. The results showed that comparing to conventional injection molding, the tensile strength and impact strength of the samples molded by vibration injection molding were also improved by 17.6 and 179.6%, respectively.

While, in the past works, many people just paid attention on the short-time mechanical properties, such as the tensile strengthen, impact strength, and so on. However, the creep behavior of PP/$CaCO_3$ mold by mechanical vibration injection molding was not investigated in the past, but the anti-creep behavior is very an important factor for any material to be used, especially these parts which will be applied the large load for long time and be asked not to deform. Therefore, our work mainly finds out a best process condition to improve the anti-creep property of PP/$CaCO_3$ mold by mechanical vibration injection molding, and analyzes how the different vibration conditions influence the creep behavior.

In this article, we used a mechanical vibration injection molding machine (Fig. 1) by utilizing a reciprocating piston. In this injection machine, the vibration force field is applied during the melting, injection and packing step of the entire molding cycle

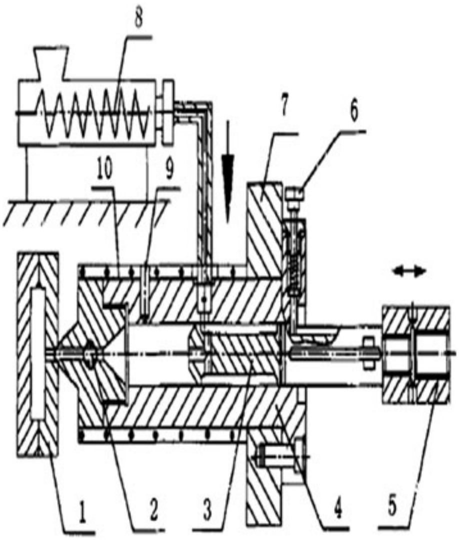

Fig. 1 Schematic of the mechanical dynamic injection molding equipment (*1* die assembly, *2* three transfixion valve, *3* injection pole, *4* hopper, *5* pitman, *6* spring pin, *7* fixed base, *8* extruder, *9* thermometer hole, and *10* heater)

by piston vibration, and the vibration frequency and vibration pressure amplitude during processing were changed, respectively. And these specimens had been applied the load of 4 MPa by using a custom-made creep apparatus (Fig. 3), then it was observed for the tensile strain of these specimens during 24 h. Finally, the reason why the anti-creep property changes will be analyzed according to the inner microstructure of polymer parts prepared under different vibration conditions. The inner microstructure of PP/$CaCO_3$ parts was investigated, based on the phase morphology and the number of the crystal grain, with aid of differential scanning calorimetry (DSC) and wide-angle X-ray diffraction (WAXD).

Experiment

Apparatus

The apparatus used in the experiment was a custom-made mechanical vibration injection molding machine. The difference of this machine from other conventional injection machines is that it applies a vibration field on injection process and packing pressure process by a mechanical force. The structure of the machine is shown schematically in Fig. 1.

From the figure, it could be found that the screw in the extruder delivered the melt material into a store holder, and the piston will be operated periodically for and after by the cylinder. At the same time, the backside of the screw was fixed in order to prevent the meld in the store hold from overflowing because of the inner strong pressure. Finally, the vibration field had been transferred to meld via the moving piston. For the mechanical vibration injection machine, the diameter of the screw was 38 mm and the *L*/*D* ratio was 20:1, where *L* is the length of the screw and *D* is the diameter of the screw.

Material

Isotactic polypropylene (iPP), supplied by the LanGang petroleum chemical, P. R. China, had a melt flow index (MFI) of 1.87 g/10 min and an M_w of 7.8×10^4. $CaCO_3$, supplied by Pengcheng Chemical Co. Ltd. P. R. China, had average particle size of 1.52 μm.

Compounding

$CaCO_3$ particles were first dried in an oven at 70 °C for 2 h and then pre-mixed with PP pellets in a tumble mixer for 5 min in a compositional ratio (30%). Because we just research about the processing condition's influence on the composites, we just choose the 30% content to research, the reason why we choose the content is because the dispersion is better in the parts, and the mechanical property may be better [14]. The pre-mixed compounds were then fed into a Keya SVF-113-380C counter-rotating twin-screw extruder with a barrel temperature of 160–190 °C was cooled in water and cut into pellet by using a pelletizer.

Sample preparation

After pelletized and dried, the blends were injected into a mold with aid of a 20 g injection molding machine. The main feature of the mechanical vibration injection molding technology was to introduce a shear field into the melt during injection stage and packing stage by a piston that moved reversibly. The processing parameters are shown in Table 1. The injection pressure amplitude is the changing pressure that the melt has been pushed into cavity with, and the pressure amplitude has been shown in Fig. 2. The vibration pressure amplitude is the pressure by which the piston in hopper (Fig. 1) injects the melt in cavity. The piston was represented by the B in the Fig. 2a, and why the piston move as the sine curve had been described in the Fig. 2a. The movement of piston is provided by the cylinder which

Table 1 Processing parameters of the mechanical vibration injection molding machine

Processing parameter	Value
Injection pressure (MPa)	60
Packing pressure (MPa)	50
Melt temperature (°C)	220
Mold temperature (°C)	50
Cooling temperature (°C)	23
Vibration frequency (Hz)	0–2.3
Vibration pressure amplitude (MPa)	0–90

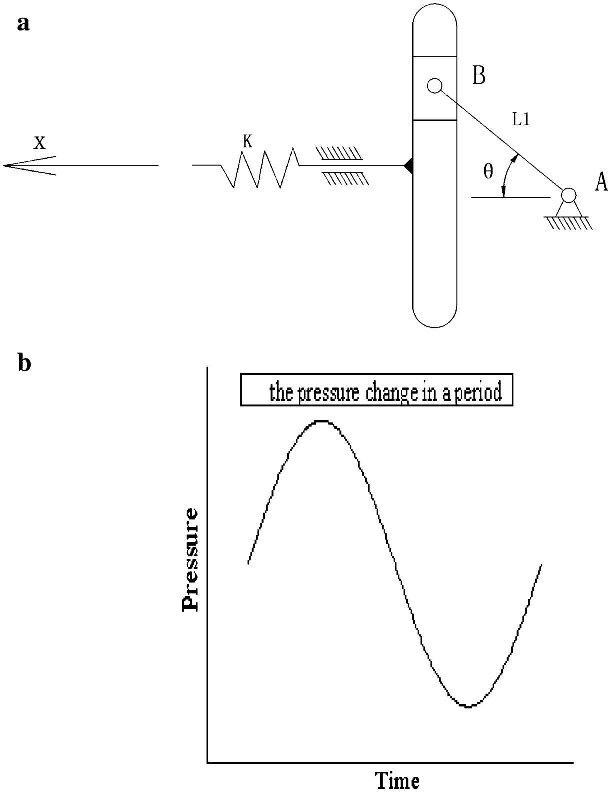

Fig. 2 **a** The schematic of piston moving. **b** The vibration pressure amplitude

gave a last changing force to the piston. In this case, filling composites are labeled by prefix “f” and “S” for frequency and vibration pressure amplitude, respectively.

Differential scanning calorimetry

The thermal analysis of the samples was conducted by using a TA 20 DSC, indium calibrated. Melting endotherms were obtained at 10 °C/min with 4–5 mg of sample in a nitrogen atmosphere, and then kept constant temperature 10 min. For the purpose of comparison with plain polymer, the crystallinity X_c of composite *i* in the composites can be normalized by the equation

$$X_c = \frac{\Delta H}{\Delta H_0}, \tag{1}$$

where ΔH is the enthalpy of fusion of the specimen mold by mechanical vibration injection molding, directly obtained from DSC, and ΔH_0 is the enthalpy of fusion of 100% crystalline polymer is 207 J/g for iPP.

WAXD measurements

The WAXD experiments were conducted by using an X’ per Pro MPDX diffractometer. The wavelength of the monochromated X-ray from Cu Kα radiation was 0.154 nm and the scanning 2θ range was from 5° to 50° with a scanning rate of 1°/min.

Tensile creep experiment

A tensile creep experiment was carried out with a custom-made creep apparatus. The two air clamps separately fix the two sides of the specimen, and then a force to stretch the sample up. On the top air clamp, there is a probe, and an infrared ray meter is near the probe, which investigates the movement of the probe, when the probe moves, then the meter will measure the distance of the movement. This distance is the tensile length of the specimen for span, which we could calculate the tensile strain according to. The equipment is shown in schematically in Fig. 3. In the experiment, the specimens were applied the load of 4 MPa for 24 h, which is 10% of the tensile strengthen. The measure temperature was room temperature (23 °C). The tensile strain has been calculated by the equation: $S = d_1/d$, where S is the strain of the sample, d_1 is the movement distance of the probe, and d is the length of the sample between top air clamp and below air clamp. Finally, the tensile creep could be directly obtained.

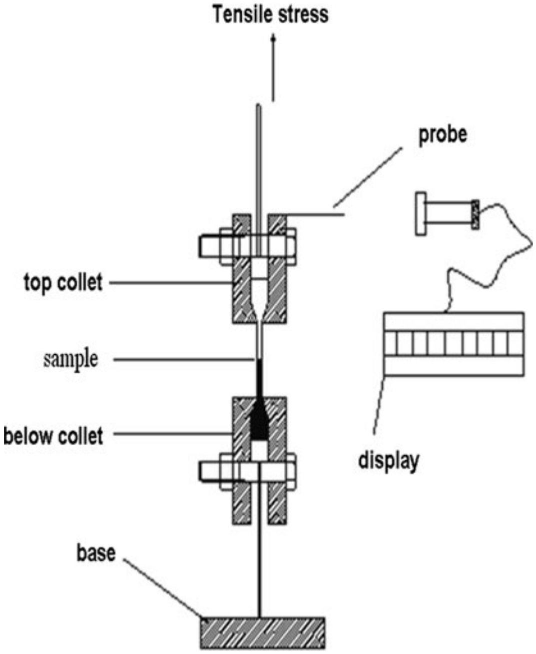

Fig. 3 Tensile creep apparatus

Discussion

The creep behavior of the PP/$CaCO_3$ prepared by vibration injection molding

It has been shown in Fig. 4a for the tensile strain of the PP/$CaCO_3$ prepared by different vibration frequencies and 50 MPa. Figure 4b is the tensile strain curve in 24 h of PP prepared at the different vibration frequencies and 50 MPa. Figure 4b shows that the tensile strain of PP/$CaCO_3$ prepared by 0.72 Hz reaches the maximum value (9.5%). When the vibration frequency exceeds the 0.72 Hz, the tensile strain decreases sharply, even it is less than that at 0.24 Hz. However, the tensile strain value decreases very slowly from 1 to 2.3 Hz.

Meanwhile, it can be observed in Fig. 5a for the tensile strain of the PP/$CaCO_3$ prepared by different vibration pressure amplitude and 0.48 Hz. Figure 5b is the tensile strain curve in 24 h of PP prepared at the different vibration pressure amplitude. With the vibration pressure amplitude increasing, the tensile strain is decreasing. The maximum value of the tensile strain is 7.8% at 50 MPa, and then the decreasing tendency is very slow from 50 to 70 MPa according to the curve. However, the decreasing slope is gradually lager, when the vibration pressure

Fig. 4 **a** The strain of PP/$CaCO_3$ samples prepared at the different vibration frequencies. **b** The strain of PP/$CaCO_3$ samples prepared at the different vibration frequencies after 24 h

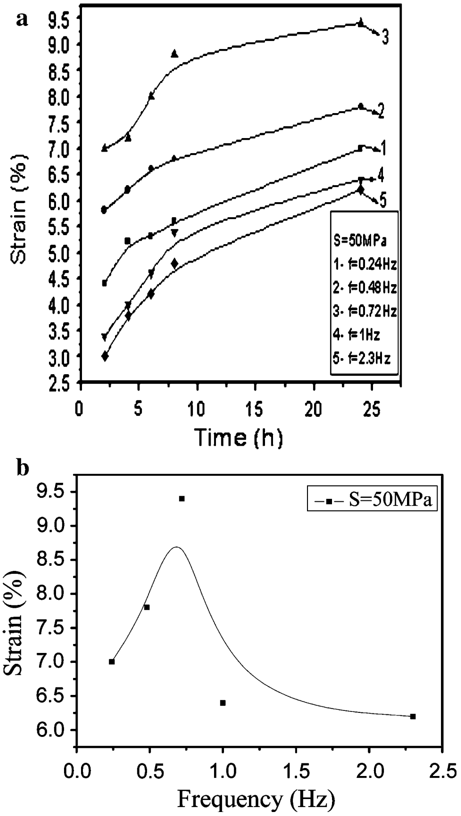

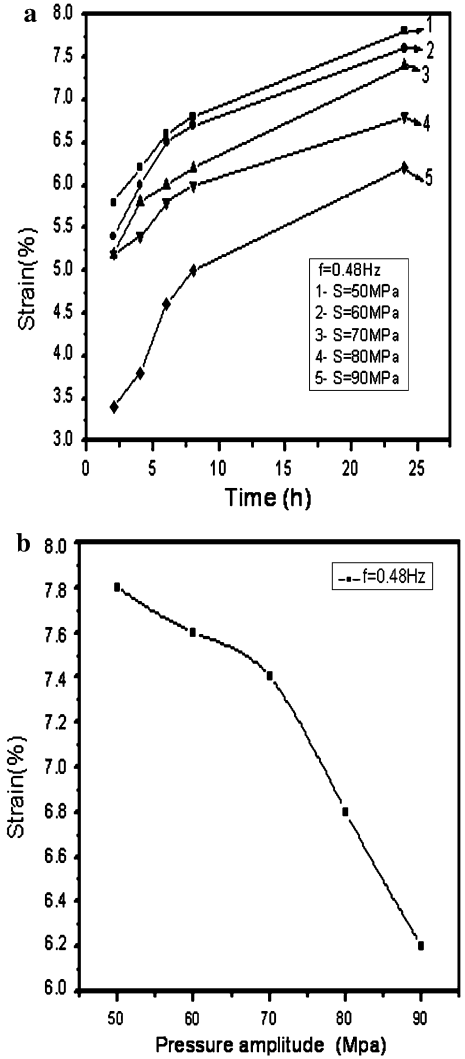

Fig. 5 **a** The strain of PP/$CaCO_3$ samples prepared at the different pressure. **b** The strain of PP/$CaCO_3$ samples prepared at the different pressure after 24 h

exceeds 70 MPa. The tensile strain value decreases from 7.4 to 6.2%, when the vibration pressure amplitude increases from 70 to 90 MPa.

According to these results, different vibration condition shows different influence on the creep behavior of PP/$CaCO_3$. For the PP/$CaCO_3$ prepared at different vibration pressure amplitude, the creep resistance increases with the vibration pressure amplitude. However, when the vibration frequency increases from 0.24 to 2.3 Hz, the creep resistance reaches the minimum at 0.72 Hz. The changes in the structure and morphologies owing to the variation of processing parameters, which results in different creep behavior of the parts mold by vibration injection molding will be discussed in the following sections.

The factors of influence on creep behavior

The creep behavior is mainly caused by the movements of the macromolecular chains in the crystalline region and amorphous region. Meanwhile, the creep behavior in the amorphous region is mainly the macromolecular chain motion, and the motion is also impacted by the crystalline region. The reason is that the macromolecular chains often pass though much lamellar, which makes the macromolecular chain to be impacted by the crystalline region. Therefore, for the semi-crystalline polymer, a macromolecular chain which exists both crystalline region and amorphous region will form a tie [17], and consequently, the plenty tie chains will form a physical cross-linking net which will limit the macromolecular chain in amorphous region motion. Then the cross-linking point is the crystalline region or crystal grain. Therefore, whether the physical cross-linking net is strong or not is decided by the number of cross-linking point. The more cross-linking points will cause stronger physical cross-linking net [17]. Finally, it can be conclude that the creep behavior in amorphous region is impacted by the number of cross-linking point.

The different creep behavior of PP/CaCO$_3$ may be caused by the different microstructure. Different vibration condition would cause different crystal structure, etc. crystal form, size of crystal grain, and crystallinity. Because the different microstructure will have huge impact on the mechanical properties, the different vibration condition will also impact the creep behavior. In the next part, the WAXD and DSC can be used to analysis the microstructure and find the reason of the different creep behavior.

The size of the crystal grain

The vibration field would change the morphologies of polymers, thus leading to improved properties [11], such as better tensile strength, impact strength, and so on. Here, WAXD and DSC were adopted to investigate the crystalline morphology of PP/CaCO$_3$ prepared at different vibration condition.

The size of the crystal grain could be gained by the Sherrer equation [18]

$$L_{hkl} = k\lambda/(\beta\cos\theta) \tag{2}$$

where L_{hkl} is the crystallite diameter (hkl), λ is the wavelength of the X-ray, θ is the Bragg angle, β is the width of the diffraction peak, and k is the Scherrer shape factor (here k is 0.9). β can be calculated by the equation: $\beta = (b^2 - b_0^2)^{1/2}$, where b is the specimen half-peak width, b_0 is the standard half-peak width, and b_0 is 0.1215°. Therefore, according to the WAXD curve, the thickness of lamellar of polymer can be obtained. It is observed that the α crystal is dominating and the β, γ crystal is very rare, so the α crystal is the main part for judging the average thickness of lamellar of PP. By studying on the α crystal, it has been known that the α crystal is skew-hexogen packing [17] and the angle of the quadrilateral of back surface of α crystal is not variable. Hence, the capacity of the crystal grain of PP will be deduced grossly from other two crystal plane thickness of the α crystal. According to the research of Wu [19], the volume of the crystal grain will be calculated as follows:

$$V = L_{(110)} \times L_{(040)} \times L_{(111)} = k\lambda / \left[(\beta(\cos\theta)_{(110)} \times (\beta(\cos\theta)_{(040)} \times (\beta(\cos\theta)_{(111)}\right], \quad (3)$$

where L is the thickness of a crystal face, β is the width of the diffraction peak, θ is the Bragg angle, and $k\lambda$ is $1.542 \times 0.9 = 1.3878$.

The size of the crystal grain of PP/CaCO$_3$ prepared at different vibration conditions

According to the WAXD curve in Fig. 6 and Table 2, there is mainly α crystal in the PP/CaCO$_3$ part prepared at different vibration frequencies. The reason may be that the CaCO$_3$ inorganic particle destroys other crystal form. Especially, some particular crystal form, which can just be got in some special condition, may be not formed.

Although analyzing the PP part by vibration injection molding and CIM and PP/CaCO$_3$ part prepared by CIM (Fig. 7), it could be found that the size of the crystal grain of PP part by CIM is larger than that of PP/CaCO$_3$, which shows that the ingronic particles may obstruct the form of the crystal, and make it not to grow larger (Fig. 7a, b). And the β peak disperses in the system of PP/CaCO$_3$ part by vibration injection molding comparing the PP part by vibration injection molding, it also shows that the ingronic filler would destroy some particular crystal form (Fig. 7b, c).

The size of the crystal grain at 0.72 Hz is larger than that at 0.24 Hz. The reason may be that the macromolecular will be easy to be close to the crystal lamellar, and fold to form crystal before the direction of the vibration force field changes, because the low frequency lead to a long period of reciprocating movement. Meanwhile, as a

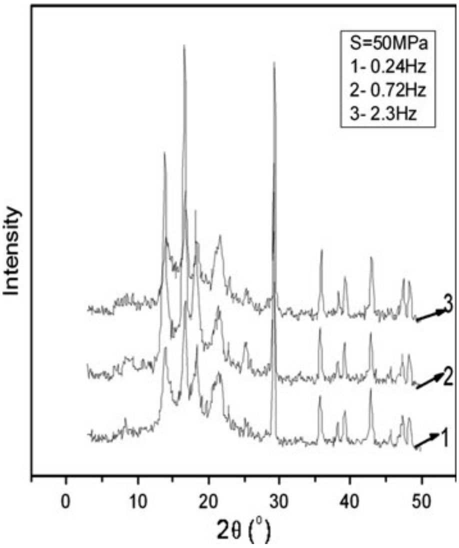

Fig. 6 The X-ray diffraction curves of the PP/CaCO$_3$ prepared at different vibration frequency and pressure amplitude of 50 MPa

Table 2 The half-peak width and diffraction angle of PP/$CaCO_3$ prepared at different vibration frequencies

	$f = 0.24$ Hz $S = 50$ MPa			$f = 0.72$ Hz $S = 50$ MPa			$f = 2.3$ Hz $S = 50$ MPa		
The crystal plane	110	040	111	110	040	111	110	040	111
Half-peak width F (°)	1.95	0.842	2.35	0.683	0.575	2.44	1.9	1.2	2.25
Diffraction angle 2θ (°)	14.2	16.8	21.2	14.2	16.8	21.2	14.2	16.8	21.2
Volume (nm^3)	126,060			541,211			101,573		

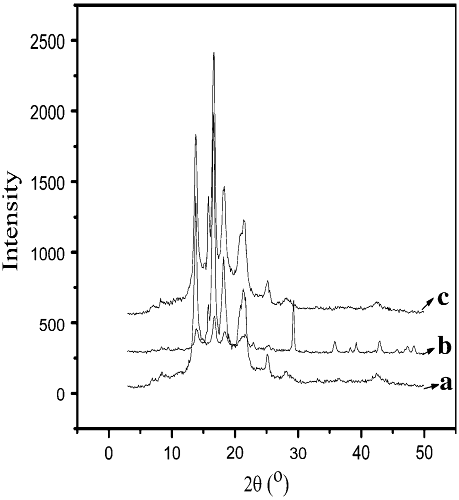

Fig. 7 The X-ray diffraction curves of PP by different injection technology. **a** PP by Conventional injection molding, **b** PP/$CaCO_3$ by conventional injection molding, **c** PP by the vibration injection molding

premise that the there are enough time for macromolecular to be close to the crystal lamellar to form crystal, when the frequency increases, and then in same time, there are more macromolecular chains which is impacted by the vibration field and is close to the crystal lamellar to form crystal, and increase the thickness of the lamellar. Because in same time, there will be more reciprocating movement vibration periods, which will impact more macromolecular chains. However, with the vibration frequency exceeding 0.72 Hz, it can be shown that the half crystal peak wide is increasing, and the increasing half-peak wide causes that the thickness of the crystal plane is decreasing gradually according to the sheerer equation [20]. Because of the piston's movement faster, there will be two different directions' force, and the directions are contrary totally as the Fig. 8. In a period, the macromolecular chains may be forced to be close to the lamellar (Fig. 8a), this force movement direction is right for macromolecular chain to form crystal. However, because the frequency is very high, which cause the very fast change of the direct of the force in filed, then and the macromolecular chains may move like the next Fig. 8b and follow the change of force field away the lamellar and before reaching the lamellar, them has been took away from the surface of lamellar. Therefore, the

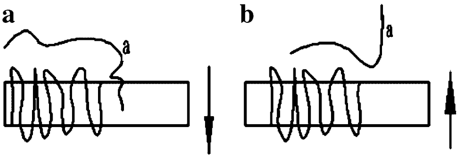

Fig. 8 The schematics of the vibration-induced subsequent growth of oriented folded chained crystal

movement will make it is more difficult for macromolecular chain to touch the lamellar and form a perfect crystal. Hence, the higher vibration frequency leads to the faster growth of crystal. However, when the vibration frequency reaches a value, it will have obvious negative influence on the crystal grow of the filling system.

According to the WAXD curve in Fig. 9 and Table 3 of the PP/$CaCO_3$ prepared at different vibration pressure amplitude, there is mainly α crystal. With the vibration pressure amplitude increasing, the crystal peak does not change basically, and then the thick of the crystal plane is also stable basically. It shows that the change of the vibration pressure amplitude does not impact the size of the crystal grain. The reason may be that no matter how strong the vibration pressure amplitude is, because of the unvaried vibration frequency, the macromolecular chains will move at same speed, which causes that may same number macromolecular chains around a crystal grain take part into the crystallization process in a time segment at same speed, so the size of the crystal grain do not have difference comparing the specimens prepared at different vibration pressure amplitude. Hence, the size of the crystal grain will not have great change. Meanwhile, when the vibration pressure is stronger, the macromolecular chains will be easier to be together to form crystal nucleus. The reason is that the stronger mechanical force may push these macromolecular chains to get closer and form more crystal nucleuses. Hence, this is also the other reason that the size of the crystal grain is very average with the vibration pressure amplitude increasing.

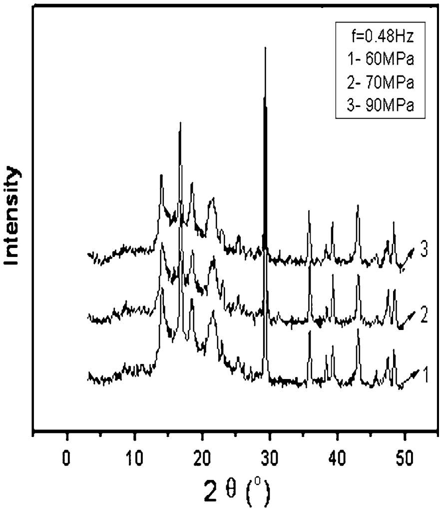

Fig. 9 The X-ray diffraction curves of the PP/$CaCO_3$ prepared at different vibration pressure amplitude and a frequency of 0.48 Hz

Table 3 The half-peak width and diffraction angle of PP/CaCO$_3$ prepared at different vibration pressure amplitude

	$f = 0.48$ Hz $S = 60$ MPa			$f = 0.48$ Hz $S = 70$ MPa			$f = 0.48$ Hz $S = 90$ MPa		
The crystal plane	110	040	111	110	040	111	110	040	111
Half-peak width F (°)	1.5	0.91	2.1	1.8	0.8	2.1	1.8	0.7	2.3
Diffraction angle 2θ (°)	14.2	16.8	21.2	14.2	16.8	21.2	14.2	16.8	21.2
The volume of crystallite (nm^3)	181,659			172,366			179,838		

The DSC curve and analysis of the PP/CaCO$_3$ prepared at different vibration conditions

According to the DSC curves, the dense of PP, the size of the crystalline region could be gained.

First, the crystallinity can be calculated from the equation [21]:

$$X = \frac{\rho_c V_1}{\rho_1 V_0}, \tag{4}$$

where X is the crystallinity, V_1 is the capacity of crystal, V_0 is the capacity of the PP, ρ_c is the density of crystalline region, and ρ_1 is the density of PP.

Second, according above equation, the percentage of the crystalline region can be calculated from the equation:

$$a = \frac{V_1}{V_0} = X\frac{\rho_1}{\rho_c}, \tag{5}$$

where ρ_c is 0.986 g/cm^3.

According to the DSC curves in Fig. 10 and Table 4 of the PP/CaCO$_3$ part prepared at different vibration frequencies and 50 MPa, the crystallinity of the PP in the filling system will be largest at 0.24 Hz. It represents that at 0.24 Hz it is easier for the molecular chain to form crystal. However, the difference of the crystallinity among the samples prepared at different vibration frequency is not very obvious. The reason is that the CaCO$_3$ particles destroy the process of crystal form of PP, which leads to the flattening of crystallinity. According to above the data, the percentage of crystal area of PP will be calculate and shown in Table 5.

According to DSC curves in Fig. 11 and Table 6 of the PP/CaCO$_3$ prepared at different vibration pressure amplitude and 0.48 Hz, the crystallinity of the PP prepared at 60 MPa is less than the crystallinity of the PP prepared at other vibration pressure amplitude. It illustrates that it is easier for molecular chain to crystallizate at 90 MPa. The main reason may be that although the molecular chain can be very difficult to go into lamellar so that the size of the crystal grain cannot grow, the vibration pressure amplitude is larger, then the movement of the molecular chain will be stronger, which causes the molecular chains touch each other close together. It results the density of the nucleus of crystal will also be larger. Hence, the crystallinity of PP will be increasing with the vibration pressure amplitude

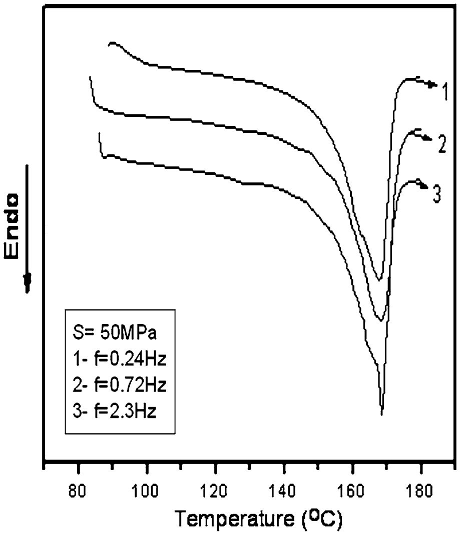

Fig. 10 The DSC curve of PP prepared at different vibration frequency and pressure amplitude of 50 MPa

Table 4 The crystallinity and the melting of PP/$CaCO_3$ prepared at different vibration frequency

	$f = 0.24$ Hz	$f = 0.72$ Hz	$f = 2.3$ Hz
Crystallinity (%)	30.76	29.26	29.55
Density of PP ρ_1 (g/cm^3)	0.8946	0.8926	0.8929

Table 5 The percentage of crystal area of PP prepared at different vibration frequency

	$f = 0.24$ Hz	$f = 0.72$ Hz	$f = 2.3$ Hz
a (%)	27.91	26.49	26.76

increasing. According to above the data, the percentage of crystal area of PP will be calculate and shown in Table 7.

The number of the crystal grain

As we known, the creep behavior is mainly impacted by the physical cross-linking degree, while the physical cross-linking degree is related with the number of the crystal grain. According to the percentage of the polymer crystal capacity from the DSC atlas and the crystal grain size from the WAXD atlas, the number of the crystal grain will be pre-estimated. The number of the crystal grain can be calculated from the equation [19]:

$$N = 1 \times X \times 10^{18}/V, \tag{6}$$

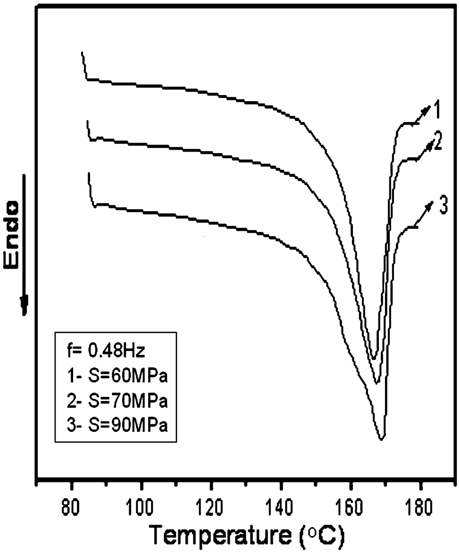

Fig. 11 The DSC curve of PP prepared at a frequency of 0.48 Hz and different pressure amplitude

Table 6 The crystallinity and melting range of PP/$CaCO_3$ prepared at different vibration pressure amplitude

	$S = 60$ MPa	$S = 70$ MPa	$S = 90$ MPa
Crystallinity (%)	26.64	28.64	32.43
Density of PP ρ_1 (g/cm^3)	0.8892	0.8918	0.8968

Table 7 The percentage of crystal area of PP prepared at different vibration pressure amplitude

	$S = 60$ MPa	$S = 70$ MPa	$S = 90$ MPa
a (%)	24.02	25.90	29.50

where the capacity is supposed as 1 mm^3, which is 10^{18} nm^3, and N is the number of the crystal grain, X is the crystallinity of PP, and V is the capacity of the average crystal grain.

According to the equation, the number of the crystal grain will be gained in same capacity.

The number of the crystal grain in the PP prepared at 50 MPa

$$N\,(f = 0.24\ \text{Hz}) = 10^{18} * 0.2791/126,060 = 2.214 * 10^{12}$$
$$N\,(f = 0.72\ \text{Hz}) = 10^{18} * 0.2647/541,211 = 4.8909 * 10^{11}$$
$$N\,(f = 2.3\ \text{Hz}) = 10^{18} * 0.2676/101,573 = 2.6346 * 10^{12}$$

Fig. 12 The comparison of the number of crystallite of PP/CaCO$_3$ prepared at different vibration frequency

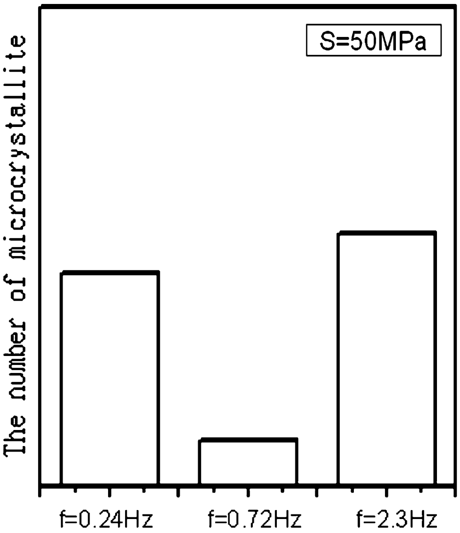

If the number of the crystal grain will be least, then it represents the physical cross-linking degree is least, and the physical cross-linking net will also be weaker relatively. Hence, less is the physical cross-linking degree; easier is the molecular chain moving [20]. Due to this reason, the macromolecular chains in the PP/CaCO$_3$ part which has fewer crystal gains may move easily relatively, relax more rapidly and endure the greater force. Comparing the crystal grain number (Fig. 12) of the PP/CaCO$_3$ part prepared at 0.24 Hz, the crystal grain number is the larger than PP/CaCO$_3$ part prepared at 0.72 Hz. It would explain that it is more difficult for the movement of the macromolecular chain of the PP/CaCO$_3$ prepared at 0.24 Hz, so it will improve the anti-creep property of the composite. As the same reason, comparing the number of crystal grain of the PP/CaCO$_3$ prepared at 2.3 Hz with that at 0.72 Hz, the number will increase again at high vibration frequency, which causes the anti-creep property becomes strong again. Therefore, the anti-creep property will be worst at 0.72 Hz.

The number of the crystal grain in the PP prepared at 0.48 Hz

$$N\,(S = 60\ \mathrm{MPa}) = 10^{18} * 0.2402/181{,}659 = 1.3223 * 10^{12}$$

$$N\,(S = 70\ \mathrm{MPa}) = 10^{18} * 0.259/172{,}366 = 1.5026 * 10^{12}$$

$$N\,(S = 90\ \mathrm{MPa}) = 10^{18} * 0.295/179{,}838 = 1.6404 * 10^{12}$$

Comparing the crystal grain number (Fig. 13) of the PP/CaCO$_3$ parts prepared at the different vibration pressure amplitude and 0.48 Hz, it can be shown that the number will increase with the vibration pressure amplitude increasing. As above explanation, it also illustrates that the physical crosslinking structure will be stronger in the high vibration pressure amplitude, and it leads to the better anti-creep property. Hence, the tensile strain at 90 MPa is less than other material in 24 h.

Fig. 13 The comparison of the number of crystallite of PP/CaCO$_3$ prepared at different vibration pressure

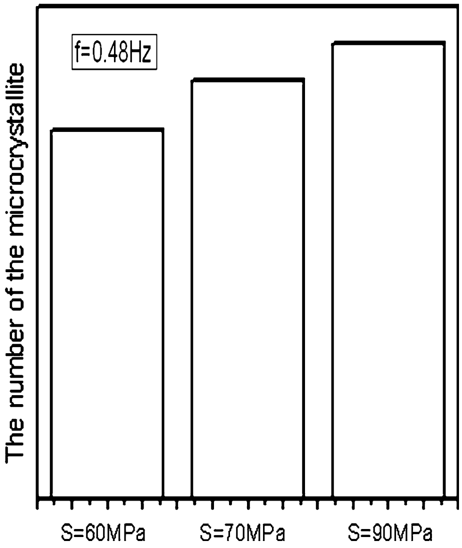

Conclusion

In this work, the creep behavior with a fixed time of a PP/CaCO$_3$ part molded by vibration injection molding has been examined. In general, the different processing conditions such as the vibration frequency, vibration pressure amplitude will cause the different creep behavior. The anti-creep property of PP/CaCO$_3$ parts by vibration injection molding increases with the vibration pressure amplitude increasing. The anti-creep property of PP/CaCO$_3$ parts by vibration injection molding is weaker with the frequency increasing, and when the vibration frequency reaches 0.72 Hz, the tensile strain of specimens reaches the maximum (9.4%). However, if the vibration frequency exceeds 0.72 Hz, the tensile strain decreases shapely with the vibration frequency increasing. The creep behavior of the PP/CaCO$_3$ article is dependent on the crystallinity and grain size of crystals. When the crystallinity is larger and the grain size of crystals is smaller, the resistance to creep is better.

References

1. Fekete E, Molnar Sz, Kim GM, Michler GH,Pukanszky B (1999) Aggregation, fracture initiation, and strength of PP/CaCO$_3$ composites. J Macromol Sci Phys 38:885–899
2. Thio YS, Argon AS, Cohen RE, Weinberg M (2002) Toughening of isotactic polypropylene with CaCO$_3$ particles. Polymer 43:3661–3674
3. Zuiderduin WCJ, Westzaan C, Huetink J, Gaymans RJ (2003) Toughening of polypropylene with calcium carbonate particles. Polymer 44:261–275
4. Chen JD, Carrot C, Chalamet Y, Majeste J-C, Taha M (2003) Rheology of poly (n-butyl methacrylate) and its composites with calcium carbonate. J Appl Polym Sci 88:1376–1383
5. Kao N, Chandra A, Bhattacharya S (2002) Melt strength of calcium carbonate filled polypropylene melts. Polym Int 51:1385–1389

6. da Silva ALN, Rocha MCG, Moraes MAR, Valente CAR, Coutinbo FMB (2002) Mechanical and rheological properties of composites based on polyolefin and mineral additives. Polym Testing 21:57–60
7. Allen PS, Bevis MJ (1986) Live-feed packing upgrades properties of molded RTP parts. Mod Plast 63:130–133
8. Allen PS, Bevis MJ (1987) Multiple live-feed injection moulding. Plast Rubber Process App l7:3–10
9. Yan Z, Shen K, Zhang J (2004) The effect of vibration injection molding on mechanical properties of polyolefin parts. J Appl Polym Sci 91:1514–1518
10. Kalay G, Bevis MJ (1997) Processing and physical property relationships in injection molded isotactic polypropylene. 1. Mechanical properties. J Polym Sci B: Polym Phys 35:241–263
11. Ibar JP (1998) Control of polymer properties by melt vibration technology: a review. Polym Eng Sci 38:1–20
12. Ibar JP (1995) Improving molding through melt-flow oscillation. Mod Plast 72:85–91
13. Weihua L, Nanqiao Z, Zhihong Z (2006) Effects of vibration force field on structure and properties of HDPE/$CaCO_3$ nanocomposites. Polym Test 25:124–129
14. Quan W, Jinping Q (2006) Mechanical properties and morphological behavior of calcium carbonate-filled polypropylene in dynamic injection molding. Polym Int 55:1330–1335
15. Liu G, Jinping Q, Ligang D (2004) Dispersion of $CaCO_3$ in melted PP under sine pulsating flow field. Eng Plast Appl 4:25–28
16. Lihui L, Jing X, Chan D (2006) Effect of vibration on the properties of PP /nano2$CaCO_3$ blends. Plast 2:11–13
17. He PS (1997) Mechanical property of polymer. University of Science and Technology of China Press, Hefei, 155 pp
18. Renjie W (1986) Modern analysis technology for polymer. Shanghai Science and Technology Press, Shanghai, 133 pp
19. Tong W, Song L, Zhao L, Wu S, Wu G (2005) Study on crystal structure of m2PE2LLD/ PE2LD blends. China Plast 19:34–38
20. Hong H, Shichun J, Lijia A (2005) Oscillation effects on the crystallization behavior of *i*PP. Polym 46:11112–11116
21. Manjun H, Weixiao C, Xixia D (2001) Polymer physics. Fudan Press, Shanghai, 367 pp